

Globally-Optimal Event Camera Motion Estimation –Supplementary Material–

A Proof of Recursive Upper and Lower Bounds

A.1 Variance (Var)

$$\begin{aligned}
l_N(\boldsymbol{\theta}) &= \frac{1}{N_p} \sum_{\mathbf{p}_{ij} \in \mathcal{P}} (I(\mathbf{p}_{ij}; \boldsymbol{\theta}) - \mu_I)^2 \\
&= \frac{1}{N_p} \sum_{\mathbf{p}_{ij} \in \mathcal{P}} \left[\sum_{k=1}^N \mathbf{1}(\mathbf{p}_{ij} - W(\mathbf{x}_k, t_k; \boldsymbol{\theta})) - \mu_I \right]^2 \\
&= \frac{1}{N_p} \sum_{\mathbf{p}_{ij} \in \mathcal{P}} \left[\sum_{k=1}^{N-1} \mathbf{1}(\mathbf{p}_{ij} - W(\mathbf{x}_k, t_k; \boldsymbol{\theta})) - \mu_I + \mathbf{1}(\mathbf{p}_{ij} - W(\mathbf{x}_N, t_N; \boldsymbol{\theta})) \right]^2 \\
&= l_{N-1}(\boldsymbol{\theta}) + a + b + c,
\end{aligned} \tag{1}$$

where $\mu_I = N/N_p$ is the mean value of $I(\mathbf{p}_{ij}; \boldsymbol{\theta})$ over all pixels (a function of $\boldsymbol{\theta}$ itself), which is constant. N_p the total number of accumulators in I . And

$$\begin{aligned}
a &= \frac{2}{N_p} \sum_{\mathbf{p}_{ij} \in \mathcal{P}} \left\{ \mathbf{1}(\mathbf{p}_{ij} - W(\mathbf{x}_N, t_N; \boldsymbol{\theta})) \left[\sum_{k=1}^{N-1} \mathbf{1}(\mathbf{p}_{ij} - W(\mathbf{x}_k, t_k; \boldsymbol{\theta})) \right] \right\} \\
b &= -\frac{2\mu_I}{N_p} \sum_{\mathbf{p}_{ij} \in \mathcal{P}} \mathbf{1}(\mathbf{p}_{ij} - W(\mathbf{x}_N, t_N; \boldsymbol{\theta})) = -\frac{2\mu_I}{N_p} \\
c &= \frac{1}{N_p} \sum_{\mathbf{p}_{ij} \in \mathcal{P}} [\mathbf{1}(\mathbf{p}_{ij} - W(\mathbf{x}_N, t_N; \boldsymbol{\theta}))]^2 = \frac{1}{N_p}.
\end{aligned} \tag{2}$$

Thus, similar to the proof in the paper, for the objective function $L_N = \max_{\boldsymbol{\theta} \in \boldsymbol{\Theta}} l_N$, we have

$$\begin{aligned}
\overline{L_N} &= \overline{L_{N-1}} + \frac{1}{N_p} - \frac{2\mu_I}{N_p} + \frac{2}{N_p} Q, \\
\underline{L_N} &= \underline{L_{N-1}} + \frac{1}{N_p} - \frac{2\mu_I}{N_p} + \frac{2}{N_p} I^{N-1}(\boldsymbol{\eta}_N^{\theta_0}; \boldsymbol{\theta}_0).
\end{aligned} \tag{3}$$

A.2 Sum of Exponentials (SoE)

$$\begin{aligned}
l_N(\boldsymbol{\theta}) &= \sum_{\mathbf{p}_{ij} \in \mathcal{P}} e^{I(\mathbf{p}_{ij}; \boldsymbol{\theta})} \\
&= \sum_{\mathbf{p}_{ij} \in \mathcal{P}} e^{\sum_{k=1}^N \mathbf{1}(\mathbf{p}_{ij} - W(\mathbf{x}_k, t_k; \boldsymbol{\theta}))} \\
&= \sum_{\mathbf{p}_{ij} \in \mathcal{P}} e^{\sum_{k=1}^{N-1} \mathbf{1}(\mathbf{p}_{ij} - W(\mathbf{x}_k, t_k; \boldsymbol{\theta})) + \mathbf{1}(\mathbf{p}_{ij} - W(\mathbf{x}_N, t_N; \boldsymbol{\theta}))} \\
&= \sum_{\mathbf{p}_{ij} \in \mathcal{P}} e^{\sum_{k=1}^{N-1} \mathbf{1}(\mathbf{p}_{ij} - W(\mathbf{x}_k, t_k; \boldsymbol{\theta}))} e^{\mathbf{1}(\mathbf{p}_{ij} - W(\mathbf{x}_N, t_N; \boldsymbol{\theta}))} \\
&= l_{N-1}(\boldsymbol{\theta}) + a + b,
\end{aligned} \tag{4}$$

where

$$\begin{aligned}
a &= e^{\sum_{k=1}^{N-1} \mathbf{1}(\boldsymbol{\eta}_N^\theta - W(\mathbf{x}_k, t_k; \boldsymbol{\theta}))} e^{\mathbf{1}(\boldsymbol{\eta}_N^\theta - W(\mathbf{x}_N, t_N; \boldsymbol{\theta}))} = e \cdot e^{I^{N-1}(\boldsymbol{\eta}_N^\theta; \boldsymbol{\theta})} \\
b &= -e^{\sum_{k=1}^{N-1} \mathbf{1}(\boldsymbol{\eta}_N^\theta - W(\mathbf{x}_k, t_k; \boldsymbol{\theta}))} = -e^{I^{N-1}(\boldsymbol{\eta}_N^\theta; \boldsymbol{\theta})} \\
\boldsymbol{\eta}_N^\theta &= \text{round}(W(\mathbf{x}_N, t_N; \boldsymbol{\theta})).
\end{aligned} \tag{5}$$

Thus, the bounds are

$$\begin{aligned}
\overline{L}_N &= \overline{L}_{N-1} + (e - 1)e^Q \\
\underline{L}_N &= \underline{L}_{N-1} + (e - 1)e^{I^{N-1}(\boldsymbol{\eta}_N^{\theta_0}; \boldsymbol{\theta}_0)}.
\end{aligned} \tag{6}$$

A.3 Sum of Suppressed Accumulations (SoSA)

$$\begin{aligned}
l_N(\boldsymbol{\theta}) &= \sum_{\mathbf{p}_{ij} \in \mathcal{P}} e^{-I(\mathbf{p}_{ij}; \boldsymbol{\theta}) \cdot \delta} \\
&= \sum_{\mathbf{p}_{ij} \in \mathcal{P}} e^{-\delta \cdot \sum_{k=1}^N \mathbf{1}(\mathbf{p}_{ij} - W(\mathbf{x}_k, t_k; \boldsymbol{\theta}))} \\
&= \sum_{\mathbf{p}_{ij} \in \mathcal{P}} e^{-\delta \cdot \sum_{k=1}^{N-1} \mathbf{1}(\mathbf{p}_{ij} - W(\mathbf{x}_k, t_k; \boldsymbol{\theta})) - \delta \cdot \mathbf{1}(\mathbf{p}_{ij} - W(\mathbf{x}_N, t_N; \boldsymbol{\theta}))} \\
&= l_{N-1}(\boldsymbol{\theta}) + a + b,
\end{aligned} \tag{7}$$

where

$$\begin{aligned}
a &= e^{-\delta \cdot \sum_{k=1}^{N-1} \mathbf{1}(\boldsymbol{\eta}_N^\theta - W(\mathbf{x}_k, t_k; \boldsymbol{\theta}))} e^{-\delta \cdot \mathbf{1}(\boldsymbol{\eta}_N^\theta - W(\mathbf{x}_N, t_N; \boldsymbol{\theta}))} = e^{-\delta} \cdot e^{-\delta \cdot I^{N-1}(\boldsymbol{\eta}_N^\theta; \boldsymbol{\theta})} \\
b &= -e^{-\delta \cdot \sum_{k=1}^{N-1} \mathbf{1}(\boldsymbol{\eta}_N^\theta - W(\mathbf{x}_k, t_k; \boldsymbol{\theta}))} = -e^{-\delta \cdot I^{N-1}(\boldsymbol{\eta}_N^\theta; \boldsymbol{\theta})}.
\end{aligned} \tag{8}$$

Thus, the bounds are

$$\begin{aligned}
\overline{L}_N &= \overline{L}_{N-1} + (e^{-\delta} - 1)e^{-\delta \cdot Q} \\
\underline{L}_N &= \underline{L}_{N-1} + (e^{-\delta} - 1)e^{-\delta \cdot I^{N-1}(\boldsymbol{\eta}_N^{\theta_0}; \boldsymbol{\theta}_0)}.
\end{aligned} \tag{9}$$

SoEaS and SoSAaS are combination loss functions, the bounds are also a combination, so we omit the derivation here.

B Application to Visual Odometry with a downward-facing Event Camera

B.1 Bounding Box Definition

We have

$$\begin{aligned} \mathbf{x}'_k &= \begin{bmatrix} -[y_k - v_0 + s\frac{f}{d}] \sin(\omega t) + [x_k - u_0 - \frac{f}{d}(\frac{v}{\omega})] \cos(\omega t) + \frac{f}{d}(\frac{v}{\omega}) + u_0 \\ [x_k - u_0 - \frac{f}{d}(\frac{v}{\omega})] \sin(\omega t) + [y_k - v_0 + s\frac{f}{d}] \cos(\omega t) - s\frac{f}{d} + v_0 \end{bmatrix} \\ &= \begin{bmatrix} a_x + b_x + c_x + u_0 \\ a_y + b_y + c_y - s\frac{f}{d} + v_0 \end{bmatrix}, \end{aligned} \quad (10)$$

where

$$\begin{aligned} a_x &= -[y_k - v_0 + s\frac{f}{d}] \sin(\omega t), \\ b_x &= [x_k - u_0] \cos(\omega t), \\ c_x &= \frac{f}{d}(\frac{v}{\omega})[1 - \cos(\omega t)], \\ a_y &= [x_k - u_0] \sin(\omega t), \\ b_y &= -\frac{f}{d}(\frac{v}{\omega}) \sin(\omega t), \\ c_y &= [y_k - v_0 + s\frac{f}{d}] \cos(\omega t). \end{aligned} \quad (11)$$

The bounding box \mathcal{P}_k^Θ is found by bounding the values of x'_k and y'_k over the intervals $\omega \in [\omega_{\min}; \omega_{\max}]$ and $v \in [v_{\min}; v_{\max}]$. Here we only consider the case $\text{abs}(\omega t) < \pi/2$. The bounding box is easily achieved if simply considering the monotonicity and different cases. There are 17 cases in total. One case is when $\omega = 0$. Given the Ackermann motion model, we then obtain

$$\begin{aligned} \underline{x}'_k &= x_k, \quad \overline{x}'_k = -x_k, \\ \underline{y}'_k &= y_k + \frac{f}{d}v_{\min}t, \quad \overline{y}'_k = y_k + \frac{f}{d}v_{\max}t. \end{aligned} \quad (12)$$

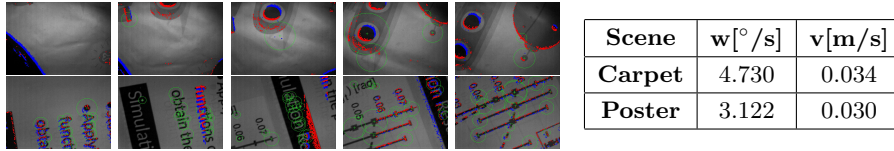
The other 16 cases are based on the monotonicity of functions. For example, if $\omega_{\min} \geq 0$, $v_{\min} \geq 0$ and $x_k \geq u_0$, $y_k \geq v_0 - s\frac{f}{d}$, the lower bound of x'_k is

$$\begin{aligned} \underline{x}'_k &= \min_{\omega} a_x + \min_{\omega} b_x + \min_{\omega, v} c_x + u_0, \quad \text{with} \\ \min_{\omega} a_x &\geq -[y_k - v_0 + s\frac{f}{d}] \sin(\omega_{\max}t), \\ \min_{\omega} b_x &\geq [x_k - u_0] \cos(\omega_{\max}t), \\ \min_{\omega, v} c_x &\geq \frac{f}{d}(\frac{v_{\min}}{\omega_{\max}})[1 - \cos(\omega_{\max}t)]. \end{aligned} \quad (13)$$

Table 1 lists \underline{x}'_k and \underline{y}'_k with ω and v arguments when the search space is $\omega_{\min} > 0$. Meanwhile \overline{x}'_k and \overline{y}'_k are obtained by ω_{\min} against ω_{\max} , and v_{\min} against v_{\max} . The other 8 cases with $\omega_{\max} < 0$ are derived by a similar strategy.

Table 1. Bounding Box Cases

Conditions			x'_k			y'_k		
			a_x	b_x	c_x	a_y	b_y	c_y
$\omega_{\min} > 0$	$v_{\min} \geq 0$	$x_k \geq u_0,$ $y_k \geq v_0 - s \frac{f}{d}$	ω_{\max}	ω_{\max}	$\omega_{\max},$ v_{\min}	ω_{\min}	$\omega_{\min},$ v_{\max}	ω_{\max}
		$x_k < u_0,$ $y_k \geq v_0 - s \frac{f}{d}$	ω_{\max}	ω_{\min}	$\omega_{\max},$ v_{\min}	ω_{\max}	$\omega_{\min},$ v_{\max}	ω_{\max}
		$x_k < u_0,$ $y_k < v_0 - s \frac{f}{d}$	ω_{\min}	ω_{\min}	$\omega_{\max},$ v_{\min}	ω_{\max}	$\omega_{\min},$ v_{\max}	ω_{\min}
		$x_k \geq u_0,$ $y_k < v_0 - s \frac{f}{d}$	ω_{\min}	ω_{\max}	$\omega_{\max},$ v_{\min}	ω_{\min}	$\omega_{\min},$ v_{\max}	ω_{\min}
	$v_{\min} < 0$	$x_k \geq u_0,$ $y_k \geq v_0 - s \frac{f}{d}$	ω_{\max}	ω_{\max}	$\omega_{\min},$ v_{\min}	ω_{\min}	$\omega_{\min},$ v_{\max}	ω_{\max}
		$x_k < u_0,$ $y_k \geq v_0 - s \frac{f}{d}$	ω_{\max}	ω_{\min}	$\omega_{\min},$ v_{\min}	ω_{\max}	$\omega_{\max},$ v_{\max}	ω_{\max}
		$x_k < u_0,$ $y_k < v_0 - s \frac{f}{d}$	ω_{\min}	ω_{\min}	$\omega_{\min},$ v_{\min}	ω_{\max}	$\omega_{\max},$ v_{\max}	ω_{\min}
		$x_k \geq u_0,$ $y_k < v_0 - s \frac{f}{d}$	ω_{\min}	ω_{\max}	$\omega_{\min},$ v_{\min}	ω_{\min}	$\omega_{\max},$ v_{\max}	ω_{\min}

**Fig. 1.** Frames from dataset *Carpet* (first row) and *Poster* (second row) and RMS errors for the different textures.

B.2 Application to Real Data and Comparison against Alternatives

Various Textures: To further analyse the robustness, we test our algorithm on datasets collected with various textures. Figure 1 presents frames from two further datasets named *Carpet* and *Poster*. The *Carpet* sequences are collected on a carpet with non-repetitive almost featureless texture, while the *Poster* sequences are collected on a poster with characters and figures for which it is easy to extract features. The estimated errors are summarised on the left of Figure 1. As can be observed, our algorithm continues have similar accuracy for the various textures in the datasets.